Large Eddy Simulations of Remote Ignition in Methane/Air mixtures behind Reflected Shock Waves

Touqeer Anwar Kashif, Janardhanraj Subburaj, Aamir Farooq
Mechanical Engineering, PSE, King Abdullah University of Science and Technology (KAUST)
Thuwal, 23955-6900, Kingdom of Saudi Arabia

1 Introduction and Motivation

Methane (CH_4), a principal component of natural gas, is increasingly recognized as a feasible alternative to conventional fossil-derived liquid fuels due to its abundant availability and reduced environmental impact in comparison to other hydrocarbon sources [1]. Furthermore, the potential application of methane as a fuel for space exploration underscores the necessity of comprehensively understanding its combustion chemistry under high-pressure and undiluted conditions. Shock tubes are essential for elucidating fuel oxidation chemistry, facilitating the development and validation of detailed chemical kinetic models. Due to inherent non-idealities in shock tube operations, diluted mixtures are often utilized for studies rather than stoichiometric fuel/air mixtures [2]. Despite these limitations, numerous datasets for ignition delay times (IDTs) at elevated pressures for methane/air mixtures have been documented in the literature. Caravaca-Vlichez and Heufer [3] compared IDTs obtained at 25 bar in various studies, unveiling discrepancies between experimental data and zero-dimensional constant volume simulations at lower temperatures. Notably, the authors observed instances of pre-ignition or mild ignition phenomena in the pressure and emission traces in the experiments exhibiting these deviations.

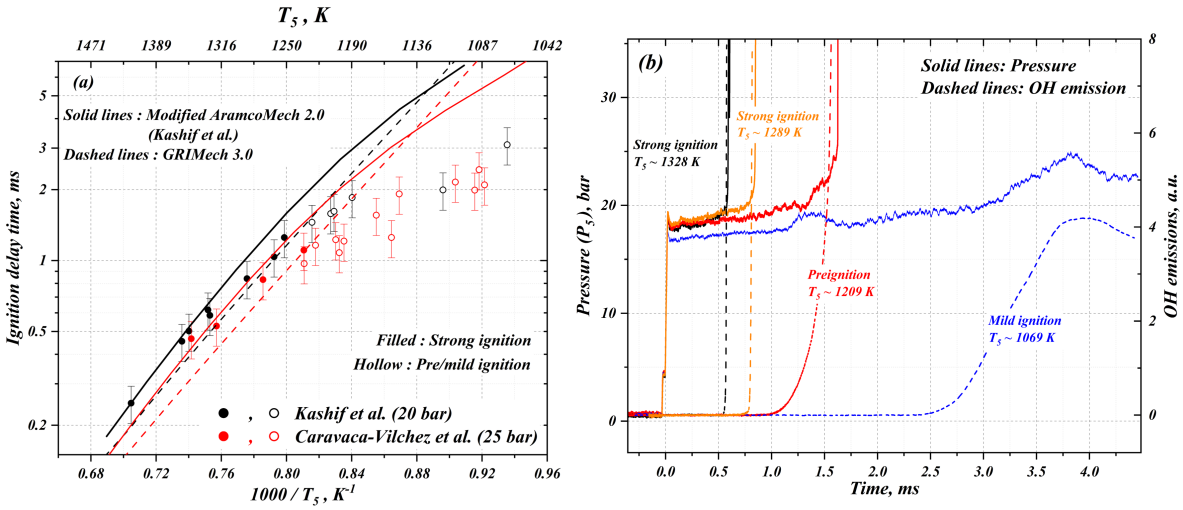

Figure 1: (a) IDT vs reciprocal of temperature for stoichiometric methane/air mixtures from [1] at 20 bar and [3] at 25 bar with emphasis on two ignition behaviors (strong and pre-ignition). (b) Pressure and OH emission traces from [1]. (Note: The IDT and pressure traces for pre-ignition case is new data.)

Correspondence to: touqeer.kashif@kaust.edu.sa

Similar observations were reported by Kashif et al. [1], and a comparison of the experimental data from the aforementioned studies ([1] and [3]) is depicted in Figure 1a. The solid symbols represent IDTs derived from strong (homogeneous) ignition experiments, whereas the hollow symbols denote experiments showing pre-ignition. The pattern of deviation of the pre-ignition affected points from the 0-D simulations (using AramcoMech 2.0 [4] and GRIMech 3.0 [5] mechanisms) is clear in both the studies. Figure 1b displays pressure and OH emission traces from the study by Kashif et al. Notably, for the red trace (for $T \sim 1209K$) classified as preignition, a gradual pressure increase is observed accompanied by a concurrent rise in OH emissions. Whereas the strong ignition cases (shown in black and orange lines) show an abrupt rise in both pressure and OH emissions. The blue trace, characterized as mild ignition, exhibits a gradual increase in pressure. However, before the ignition front transitions into a global ignition, the expansion waves terminate the test time.

Caravaca-Vilchez et al. identified regimes susceptible to pre-ignition by applying the Sankaran criteria [3], which assumes the existence of a nascent flame kernel and aims to determine if the kernel affects the global IDT considering various parameters such as flame speed, and IDT sensitivity on temperature. The origin of these flame kernels is hypothesized to stem from hot-spots due to various non-idealities within the shock tube, such as diaphragm fragments, interactions between the reflected shock wave and the boundary layer, or temperature gradients in the core shocked gas. This study attempts to numerically ascertain the precise origins of these hot-spots that catalyze the ignition in methane/air mixtures. While several numerical investigations have explored non-ideal ignition phenomena, there is no study on remote ignition characteristics in methane mixtures to the best of author's knowledge. The ensuing section will list the advantages of the current numerical methodology over existing approaches.

2 Numerical methods and conditions

In the current study, the high-pressure shock tube (HPST) facility at KAUST is numerically simulated using a commercial CFD software, CONVERGE CFD. The computational domain replicates the symmetric upper half of the shock tube, consisting of a 2.6 m driver and a 7.16 m driven section, treated as a two-dimensional domain. All boundaries are modeled as isothermal walls maintained at 294 K, except for the center-line, which is treated as a symmetry boundary. The diaphragm opening time and profile, derived from our prior work [8], are modeled with a simplified hinge mechanism at the top wall. The driver gas is comprised of Helium and driven gas is a stoichiometric CH_4/Air gas at with pressure conditions tabulated in Table 1.

Table 1: Conditions for the numerical tests conducted, with IDTs derived from monitoring the peak temperature of the reflected shocked gas and pressure at the endwall.

Case	P_4, bar	P_1, Torr	T_5, K	P_5, bar	IDT, ms		Ignition type
					Remote	Endwall	
A1	26.2	210	1349	18.7	0.35	0.38	Strong
A2	26.2	230	1313	19.4	0.548	0.561	Strong
A3	24.13	250	1248	19.1	0.821	0.929	Preignition
A4	24.13	270	1219	19.6	0.885	1.154	Preignition
A5	24.13	292	1189	20.2	0.925	1.223	Preignition
A6	24.13	315	1161	20.7	1.182	1.711	Preignition

The simulation methodology involves a two-fold approach. Initially, k-ω SST RANS simulations are conducted to capture the diaphragm opening process and the subsequent formation and propagation of the incident shock wave (ISW) along the driven section. This method, previously validated in [8 - 9],

accurately represents the effects of diaphragm opening delay and shock wave attenuation. Upon the ISW reaching the end of the driven section, data from this simulation are mapped onto a subsequent Large Eddy Simulation (LES) to simulate the shock reflection process. The mapped solution has information on extent of axial gradients induced due to shock attenuation and the boundary layer thickness. The second stage (LES) focuses on non-idealities in the driven gas with a finer grid (62.5 microns). Unlike RANS, LES is capable of resolving the complexities associated with the bifurcation of the reflected shock wave (RSW) due to its interaction with the boundary layer. GRIMech 3.0 is used as a chemical kinetic mechanism to capture the ignition event of methane in the CFD simulation. While Lipkowicz et al.'s [6] work on LES of H_2 mixtures at 1 bar offers a parallel to this study, it lacks specific discussions on the extent and impact of ISW attenuation. To our knowledge, this study is the first to simulate the entire shock tube dynamics comprehensively, including phenomena such as diaphragm opening, shock attenuation, RSW interaction with the boundary layer, and the detailed chemistry of methane/air mixtures.

3 Results and Discussion

The IDTs derived from CFD simulations for the mixtures specified in Table 1 are depicted in Fig. 2a. The data points are categorized into two types: cyan-filled points ($IDT_{endwall}$), which represent IDTs determined from the pressure rise observed 1 cm from the driven end wall, and black-filled points (IDT_{remote}), which correspond to the onset of remote ignition (or deflagration) identified by the increase in maximum temperature of the reflected shocked gas. In cases A1 and A2, the definitions of IDTs coincide, aligning closely with the zero-dimensional (0-D) CHEMKIN predictions (represented by the black solid line), indicative of a homogeneous ignition behavior. Conversely, for cases A3 through A6, $IDT_{endwall}$ exhibits notable deviations from the 0-D predictions, mirroring experimental findings. Notably, in all these cases, IDT_{remote} consistently registers lower than the IDTs recorded at the end wall, underscoring a distinct ignition dynamic for these cases.

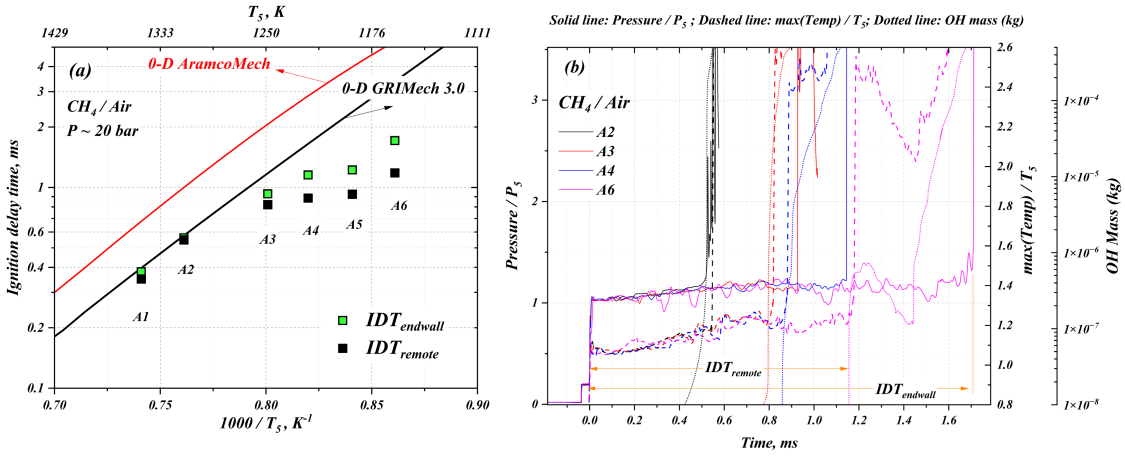

Figure 2: (a) IDT vs reciprocal of temperature from numerical simulations showing both IDTs acquired from endwall and the onset of remote ignition. (b) Temporal evolution of pressure at the endwall, maximum gas temperature, and OH mass from CFD.

In Fig. 2b, the temporal evolution of pressure at the end wall, maximum temperature, and OH mass are depicted for cases A2, A3, A4, and A6. Notably, in the strong ignition case (A2 - represented by black traces), the onset of pressure rise coincides with increases in temperature and OH mass. Conversely, for

cases A3, A4, and A6, temperature and OH mass increases precede the pressure rise at the end wall, suggesting the occurrence of remote ignition events. This earlier rise in OH mass relative to the pressure is consistent with experimental observations shown in Fig. 1b.

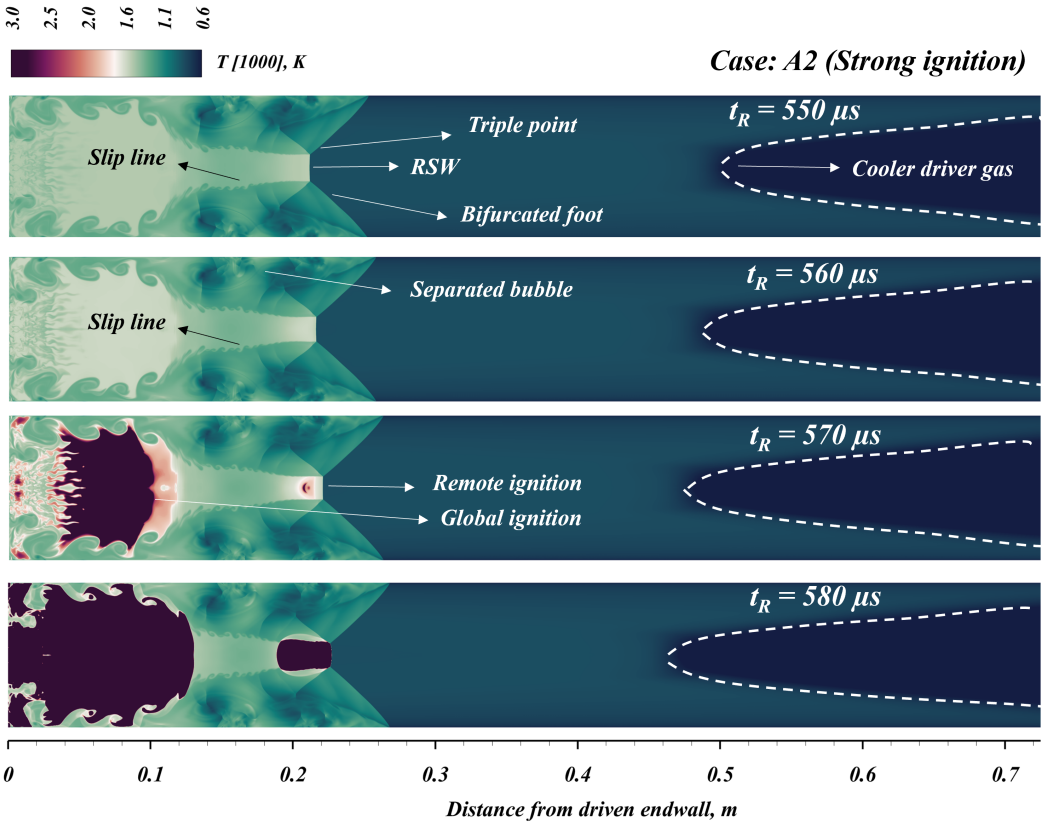

Figure 3: Evolution of the temperature in the reflected shock region in case A2 showing the remote and global ignition regions.

To illustrate the ignition locations, temperature contours are depicted in Figs. 3 and 4 a few hundred microseconds after shock reflection. Fig. 3 (for case A2) displays a temperature contour at 550 μsecs post-reflection, showing the reflected shock wave (RSW) advanced to approximately 0.2 m and undergoing significant bifurcation. This bifurcation occurs when the boundary layer fluid lacks the momentum to traverse through the RSW, resulting in flow reversal and separation at the walls, thereby splitting the RSW into a bifurcated shock with two oblique shocks emanating from a triple point [7]. A slip line delineates the flows processed by the planar and bifurcated RSWs, with the incoming contact surface (CS) indicated by dashed lines.

By t_R = 560 μsecs, there is a noticeable temperature rise across the gas slug near the end wall, leading to auto-ignition at t_R = 570 μsecs. Concurrently, a remote ignition event occurs approximately 0.2 m from the end wall, where the gas, although processed later by the RSW, ignites earlier due to elevated temperatures from shock bifurcation and attenuation-induced temperature gradients in the incident shocked gas.

For case A3 (Fig. 4), at t_R = 745 μsecs, the RSW is positioned approximately 0.3 meters downstream, where its bifurcated foot has nearly engulfed the entire RSW. Notably, regions of higher temperature develop away from the end wall. By t_R = 845 μsecs, the RSW interacts with the CS, and the formation of a secondary normal shock behind the main RSW is also observed. Immediately behind this second

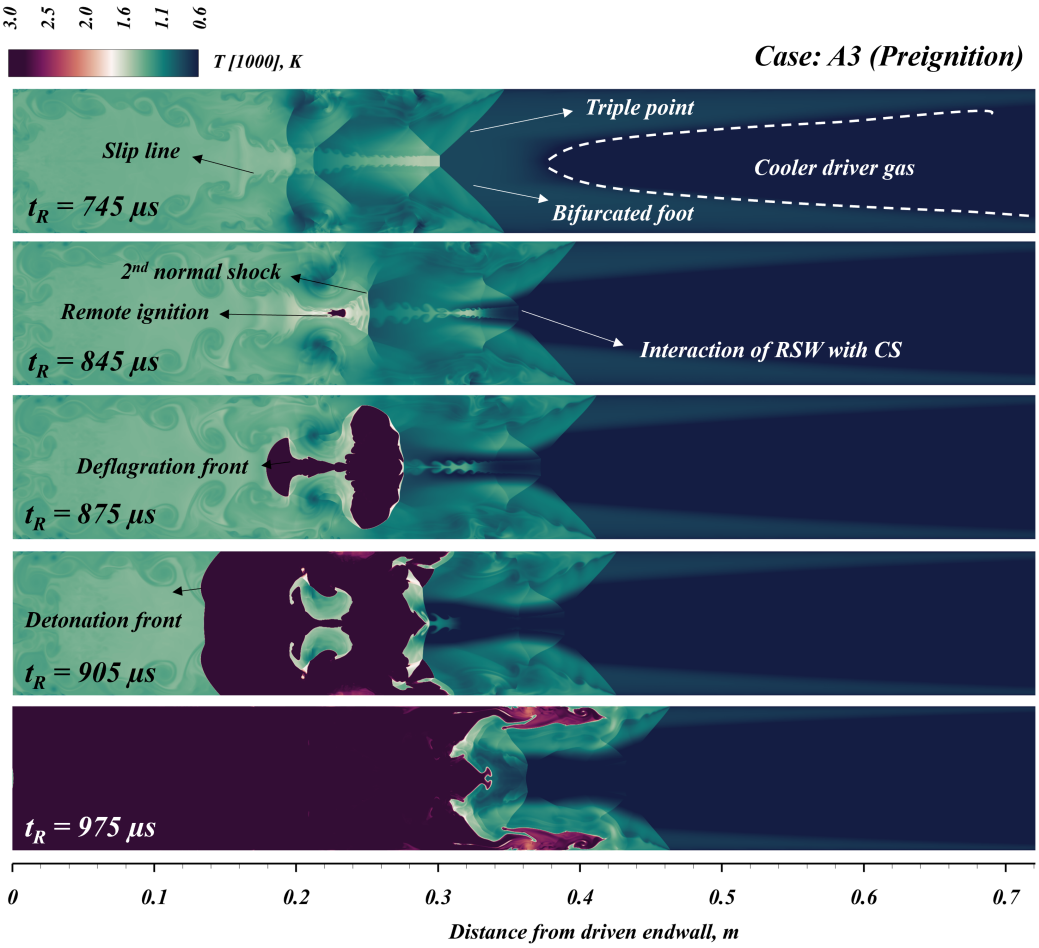

Figure 4: Evolution of the temperature in the reflected shock region in case A3 showing the remote ignition developing into a detonation wave.

shock, a distinct remote ignition event is observed. Approximately 30 μsecs later, depicted in the third panel, this ignition evolves into a deflagration wave that begins to consume the unburnt gas. By t_R = 905 μsecs, the deflagration escalates into a detonation, completely consuming the mixture, a process also evidenced in the final panel at t_R = 975 μsecs.

In summary, both cases A2 and A3 exhibit remote ignition events; however, for A2, a strong homogeneous ignition follows almost instantaneously, with minimal influence from the remote ignition. In contrast, for A3, the mixture does not ignite homogeneously; instead, there is a visible development and progression of a deflagration wave that originates away from the end wall and ultimately consumes the entire mixture. Similar behaviors are observed in cases A4 through A6. While the temperature and pressure at the ignition locations for these cases are qualitatively known to be higher than those at the end wall, quantitative analysis will be pursued in future work.

4 Summary and Future work

The numerical simulations performed in this study capture the pre-ignition phenomena observed in experiments with stoichiometric methane/air mixtures. These simulations employed a two-stage computational approach: RANS simulations initially captured the formation and propagation of the incident

shock wave, followed by LES simulations that detailed the complex interactions of the reflected shock wave with the boundary layer and other non-idealities within the reflected shocked gas. The results highlight a significant deviation in ignition delay times (IDTs) from the predictions of 0-D models, which aligns with experimental observations at lower temperatures. This deviation is primarily attributed to remote ignition events occurring away from the driven end wall, triggered by intricate flow dynamics and thermal stratification. These remote ignitions evolve into deflagration flames that consume the entire mixture before it auto-ignites. This study will be expanded to explore the behavior of oxygenated methane and hydrogen mixtures under similar conditions. Additionally, the effects of CO_2 dilution on the ignition phenomena will also be investigated.

4 Acknowledgments

This work was sponsored by the baseline funds of KAUST. All simulations were performed on KAUST Supercomputing Laboratory's (KSL) Shaheen III supercomputer. Convergent Science provided CONVERGE licenses and technical support.

References

[1] Kashif, T.A., AlAbbad, M., Figueroa-Labastida, M., Chatakonda, O., Kloosterman, J., Middaugh, J., Sarathy, S.M. and Farooq, A., 2023. Effect of oxygen enrichment on methane ignition. Combustion and Flame, 258, p.113073.

[2] Petersen, E.L., 2009. Interpreting endwall and sidewall measurements in shock-tube ignition studies. Combustion science and technology, 181(9), pp.1123-1144.

[3] Caravaca-Vilchez, J. and Heufer, K.A., 2023. New insights into the pre-ignition behavior of methane behind reflected shock waves. Shock Waves, 33(4), pp.315-328.

[4] Zhou, C.W., Li, Y., Burke, U., Banyon, C., Somers, K.P., Ding, S., Khan, S., Hargis, J.W., Sikes, T., Mathieu, O. and Petersen, E.L., 2018. An experimental and chemical kinetic modeling study of 1, 3-butadiene combustion: Ignition delay time and laminar flame speed measurements. Combustion and Flame, 197, pp.423-438.

[5] Smith, G.P., 1999. GRI-Mech 3.0. http://www. me. berkley. edu/gri_mech/.

[6] Lipkowicz, J.T., Nativel, D., Cooper, S., Wlokas, I., Fikri, M., Petersen, E., Schulz, C. and Kempf, A.M., 2021. Numerical investigation of remote ignition in shock tubes. Flow, Turbulence and Combustion, 106, pp.471-498.

[7] Weber, Y.S., Oran, E.S., Boris, J.P. and Anderson Jr, J.D., 1995. The numerical simulation of shock bifurcation near the end wall of a shock tube. Physics of Fluids, 7(10), pp.2475-2488.

[8] Kashif, T.A., Subburaj, J., and Farooq, A., 2025. On the flow characteristics in the shock formation region due to the diaphragm opening process in a shock tube. arXiv preprint arXiv:2501.13531.

[9] Kashif, T.A., Subburaj, J., Khan, M.Z.A. and Farooq, A., 2024. Influence of Diaphragm Dynamics on Shock Wave Propagation in Double-Diaphragm Shock Tubes. arXiv preprint arXiv:2412.14530.